Rapid Communications | Editors' Suggestion

Nonlinear resonances generate large-scale convection cells in phase space

Fan Wu,[1] Dmitri Vainchtein,[2,3] and Anton Artemyev[4,3]

[1]*Key Laboratory of Traffic Safety on Track, Ministry of Education, School of Traffic & Transportation Engineering, Central South University, Changsha 410075, Hunan, China*

[2]*Nyheim Plasma Institute, Drexel University, Camden, New Jersey 08103, USA*

[3]*Space Research Institute, Moscow 117997, Russia*

[4]*Institute of Geophysics and Planetary Physics, University of California, Los Angeles, California 90095, USA*

(Received 6 November 2018; published 5 February 2019)

It is well known that resonance phenomena can destroy adiabatic invariance and cause chaos and mixing. In the present Rapid Communication, we show that a nonlinear wave-particle resonant interaction may do the opposite—generate large-scale coherent structures in phase space. The combined action of the drift due to nonlinear scattering on resonance and trapping (capture) into resonance creates a convection cell-like structure, where the areas of particle acceleration and deceleration are macroscopically separated. At the same time, nonlinear scattering also creates a diffusion that cause mixing on and between the energy levels.

DOI: 10.1103/PhysRevE.99.020201

Convection cells and large-scale coherent structures are common in the physical space of fluid systems. However, similar structures in the phase space of Hamiltonian systems are much more rare [1–3]. In the present Rapid Communication we introduce a simple system of charged particles moving in a nonuniform magnetic field in the presence of an electrostatic wave. In many plasma systems, charged particle resonant interactions with electromagnetic waves represent the only way for an efficient energy exchange between particle populations. For coherent resonant interactions, particles can spend a long time within the resonance and their dynamics becomes much more complicated than just a diffusion in phase space. The first study of mixing and chaos due to resonances was done by Feingold and co-workers [4–6], who recognized that mixing is caused by the breakdown of adiabatic invariance near surfaces where the frequency of the perturbation is in resonance with the frequency of the unperturbed flow. Many examples of chaotic advection and mixing in fluids in the presence of resonances can be found in Ref. [7]. Recently, the nonlinear wave-particle interaction became one of the main approaches to the quantitative description of plasma processes in magnetospheres [8–12]. Our analysis is based on modeling charged particle motion in an effective potential generated by a combination of Lorentz forces from the background magnetic field and wave electromagnetic field. We show that particles interacting with such potentials may form large-scale convection cells in *phase* space. The internal structure of these cells and their evolution due to a particle exchange between trapped and nontrapped (transient) populations determine the wave dumping and growth, particle acceleration and deceleration, and many other important wave characteristics. In a classical problem of nonlinear Landau damping, the trapped phase-space region is assumed to be uniformly filled, and thus the events of particle trapping and escape can influence the wave dynamics [13,14]. In many systems, effects related to the formation and evolution of large-scale structures control the primary wave dynamics and secondary wave formation [15–18].

Here, we present a simple setting where nonlinear resonance phenomena create a phase-space convection cell. We start with the main equations of the wave-particle system and introduce the separation of timescales. Then we define the resonance and describe scattering at resonance and trapping (capture) into resonance at a single crossing. After that we describe the structure of the convection cell, and estimate the timescale of mixing and the period of the convection cell. Finally, we propose a kinetic Fokker-Plank-type equation that describes the leaking of particles from the cell.

A dimensionless Hamiltonian of a charged particle moving in a double-well potential in the presence of a fast wave is

$$H = \tfrac{1}{2}p_y^2 + U(y) + \beta \sin \chi\varphi,$$
$$U(y) = (\alpha^2 y^2 - 1)^2/8\alpha^2, \quad \varphi = y - ut. \tag{1}$$

Here, χ, u, and β are the wave number, phase speed, and amplitude of the wave, respectively. We assume that the wave is short, $\chi = 30 \gg 1$, and weak, $\beta = 0.1 \ll 1$. The other parameters are $\alpha = 0.1$ and $u = 1$. The minimum possible value of energy, $H_{\min} = 0$, is at the bottom of either of the two potential wells; $H_C = 1/(8\alpha^2) = 12.5$ is the value of energy at the potential barrier at $y = 0$. The unperturbed system is illustrated in Fig. 1. The separatrix S separates the motion inside one of the two wells from the motion in the top domain.

The smallness of $1/\chi \ll 1$ introduces a separation of timescales: φ is fast, while (y, p_y) and H are slow. In the first approximation, we can average Hamiltonian (1) over the fast phase, which is effectively equivalent to omitting the term $\beta \sin(\chi\varphi)$ in (1): $H_{\rm av} = p_y^2/2 + (\alpha^2 y^2 - 1)^2/8\alpha^2$. As $H_{\rm av}$ does not depend explicitly on time, it is an integral of the averaged system. In exact system (1), the value of H is approximately conserved (with the accuracy of order β) everywhere, where the separation of timescales is valid and the method of averaging works. The averaging fails when the rate of change of φ vanishes on the line called a *resonance*:

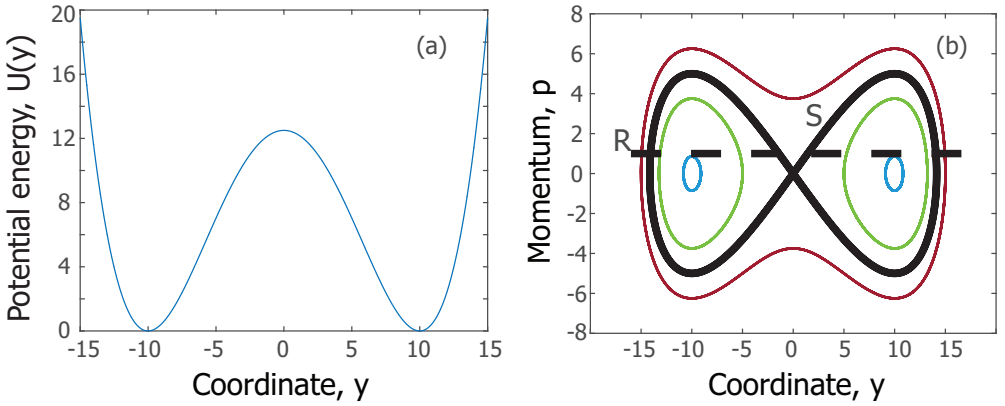

FIG. 1. The unperturbed system: (a) Profile of the potential energy. (b) Phase portrait.

$d\varphi/dt = p_y - u = 0$ [dashed line R in Fig. 1(b)]. The dynamics of particles that intersect the resonance is drastically different from that of the particles that do not intersect it. Most particles cross the resonance twice on each period of the fast motion. There are two kinds of exceptions. Particles near the bottom of the two wells ($H < H_{\min} = 0.5$) do not cross the resonance at all [two smallest circles in Fig. 1(b)]; those just above the separatrix S cross the resonance four times. Every time a particle crosses a resonance, the value of energy H changes. There are two main resonance phenomena: capture (trapping) into resonance and scattering on resonance (see, e.g., Ref. [12] and references therein).

During most of the resonance crossings, the energy of a particle changes only slightly. This process is called scattering on resonance. It follows from, e.g., Refs. [12,19] and references therein, that the change of the energy is

$$\Delta H(\xi, H) = -u\sqrt{\beta}\sqrt{2a}\int_{-\infty}^{\tilde{\varphi}_*} \frac{\cos\tilde{\varphi}\, d\tilde{\varphi}}{\sqrt{2\pi\xi + \tilde{\varphi} - a\sin\tilde{\varphi}}}, \quad (2)$$

where $\tilde{\varphi} = \chi\varphi$, $a = \beta\chi/A$, and $A = A(H) = \partial U/\partial y = y_R(\alpha^2 y_R^2 - 1)/2$. The value of A is computed at the resonance crossing: $H = u^2/2 + (\alpha^2 y_R^2 - 1)^2/8\alpha^2$. In (2), $\tilde{\varphi}_*$ is the value of $\tilde{\varphi}$ at the resonance crossing, and $2\pi\xi = \tilde{\varphi}_* - a\sin\tilde{\varphi}_*$. The value of ξ is a very sensitive function of the initial conditions: Even small, order β, changes in the initial conditions result in significant changes in ξ (see, e.g., Ref. [12] and references therein). For multiple consecutive scatterings, ξ can be treated as a random variable uniformly distributed on (0,1) (see a numerical verification of this assumption in Ref. [20]). Correspondingly, ΔH becomes a random variable as well.

The statistical properties of ΔH depend on the value of a. The average value and the second moment of ΔH are

$$\langle\Delta H\rangle(H) = \int_0^1 \Delta H(\xi, H)d\xi,$$
$$\langle(\Delta H)^2\rangle(H) = \int_0^{2\pi} [\Delta H(\xi, H) - \langle\Delta H\rangle]^2 d\xi. \quad (3)$$

It was shown in Ref. [21] that when $a > 1$, $\langle\Delta H\rangle$ is finite, and when $a < 1$, $\langle\Delta H\rangle = 0$; $\langle(\Delta H)^2\rangle$ is always finite.

Besides scattering, particles may be trapped (captured) into resonance. Trapping is possible if $a > 1$ and $da/dt > 0$ along the trajectory. In the current system, particles can be captured on the left walls in both wells. It was shown in, e.g., Refs. [12,22,23] that trapping can be considered as a random process. While for every given particle approaching the resonance it can be predicted whether or not it will be trapped (provided trapping is possible), this trapped-or-not-trapped transition is very sensitive to initial conditions. Thus, for multiple particles and multiple passages through resonance, it is reasonable to consider trapping as a probabilistic process. The method of computing the probability of trapping $\Pi(H)$ is presented in several papers (see, e.g., Refs. [12,24] and references therein).

Once a particle is trapped into resonance, its dynamics is integrable and predictable. The trapped particles move for a while with the wave: They are transported along the resonance and then are released from resonance on the right walls. The value of the energy at the release from resonance can be computed explicitly [25]. The energy input-output function is presented in Fig. 2, where we used $H\,\mathrm{sgn}(y)$ instead of H to distinguish between the left and right wells. In the left well, for $-H < -H_{lr} \approx -2$, particles are transported to the right

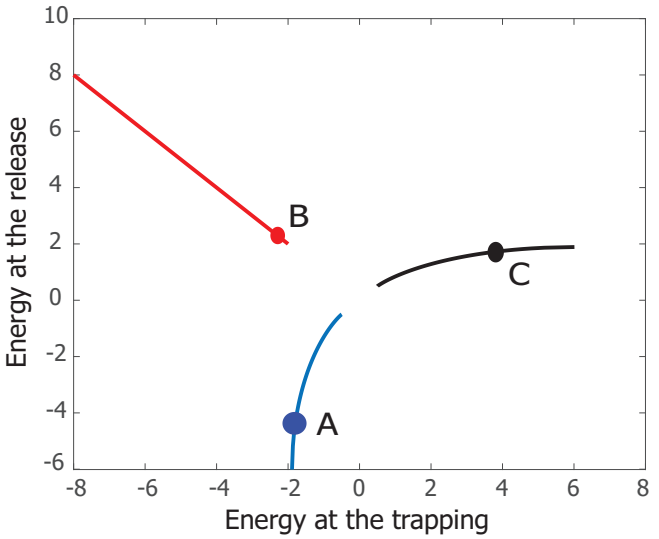

FIG. 2. Trapping (capture) into resonance: input-output function. Horizontal axis: $H\,\mathrm{sgn}(y)$ at the trapping; vertical axis: $H\,\mathrm{sgn}(y)$ at the release. Note that the energy H is multiplied by $\mathrm{sgn}(y)$. Thus the left and the right wells corresponds to $H\,\mathrm{sgn}(y) < 0$, and $H\,\mathrm{sgn}(y) > 0$, respectively.

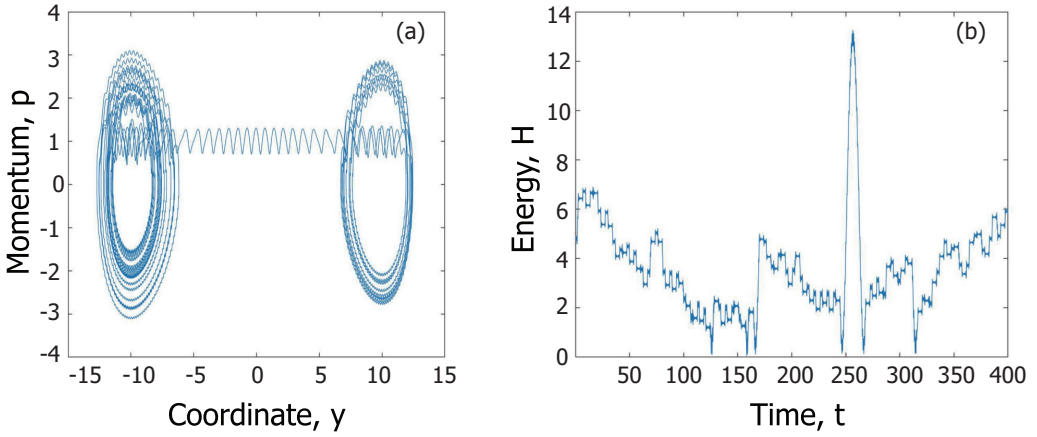

FIG. 3. Trapping (capture) into resonance. (a) Phase portrait. (b) Energy evolution.

wall of the right well (L-R capture). From the symmetry of the potential well with respect to the axis $x = 0$, in this case the energy does not change. This trapping corresponds to the red, top left, line in Fig. 2. For $0 < H_{tr} < H_{lr}$, particles are transported to the right wall of the left well (L-L capture). In this case, the energy grows (the blue, bottom left, line in Fig. 2). In the right well, all the particles captured at the left wall are transported to the right wall. The energy decays (the black, top right, line in Fig. 2).

An interval of the phase trajectory containing all three types of trapping is presented in Fig. 3. First, the particle is trapped [at $t \approx 170$ in Fig. 3(b), the outer spiral in the left well in the left panel in Fig. 3(a)] in the left well and released in the left well (point A in Fig. 2). The second time the trapping occurs at a higher value of the energy [at $t \approx 245$ in Fig. 3(b), the long spiral in Fig. 3(a)], and the particle is transported to the right well (point B in Fig. 2). The third trapping [at $t \approx 320$ in Fig. 3(b), the outer spiral in the right well in Fig. 3(a)] moves the particles from the left wall of the right well to the right wall (point C in Fig. 2).

The medium-time behavior of any given particle consists of successive motion in three distinct domains: the right well, the left well, and the top domain (above the barrier). A characteristic dynamics is illustrated in Fig. 4(a). In the right well, the value of energy grows on average, resulting in an upward advection in phase space. Then the particle enters the top domain ($t \approx 120$) where there is no drift, just a diffusion. In terms of energy, particles can go up—there is no upper bound—or down. Most of the particles spend some time in the top domain ($t \approx 120$–400). If they go down to the right well (e.g., $t \approx 200$), advection kicks them back immediately to the top domain. However, if a particle goes down the left well ($t \approx 400$), advection takes it down ($t \approx 400$–900). Near the bottom, trapping into resonance becomes possible. While the energy is not too small, above H_{lr}, trapping takes the particle from the left well to the right well: the L-R trapping. Once below H_{lr}, trapping keeps the particle inside the left well: the L-L trapping. However, the energy at the release from the L-L trapping is larger than H_{lr}. Therefore, the L-R trapping becomes possible again. The particle oscillates near the bottom of the left well undergoing the downward drift and the upward L-L trappings ($t \approx 900$–1900) until finally the L-R trapping occurs ($t \approx 1900$). After that the particle is transported to the right well and the whole process repeats again.

The structure of the resulting convection cell is illustrated in Fig. 4(b). Different colors correspond to the average value of the change of energy on a given energy level due to

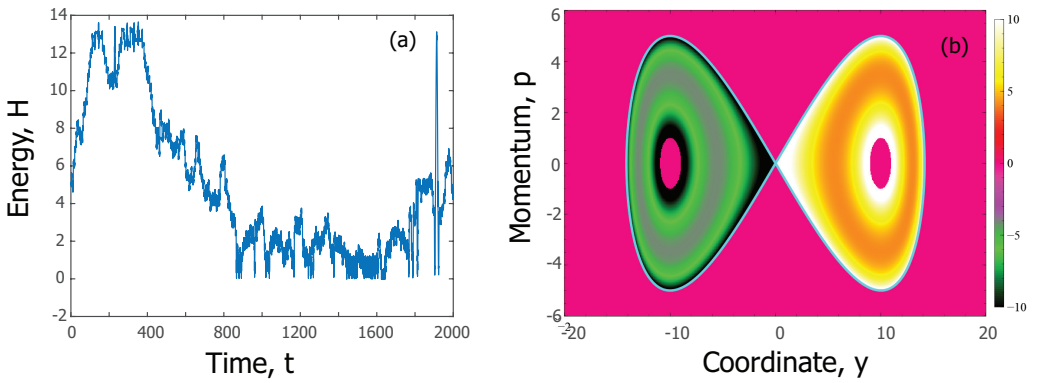

FIG. 4. Medium-time evolution. (a) Trajectory of a single particle: From the right well, up to the top well, down the left well, and transfer by capture into resonance to the right well, and starting up again. (b) The average change of energy.

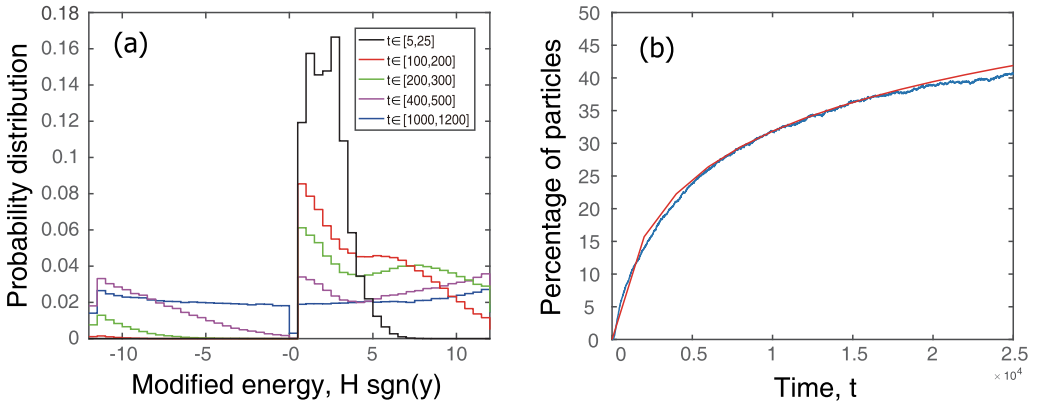

FIG. 5. Evolution of a particle ensemble. (a) Histograms of the PDF for different values of time. From the initial distribution in the right well (black curve), over the top, to the left well. Note that the axis is the energy H multiplied by sgn(y). At $t \approx 100$, the particles are in the right well; at $t \approx 250$, particles fill the right well and start coming into the left well; at $t \approx 500$, particles fill the left well; at $t \approx 1000$, particles essentially uniformly fill both bottom wells. (b) The percentage of particles in the upper domain above $H = 15$. The red curve is obtained by solving PDE (5) for the PDF, and the blue curve is the aggregation of explicit simulation of 20 000 particles governed by (1).

scattering. The average change is positive in the right well, and negative in the left well. In the upper domain the average energy change is zero. There are also regular domains at the very center of the two bottom cells, where particles do not intersect the resonance at all.

To describe mixing between the wells and the evolution of the ensemble of particles, we introduced a probability distribution function (PDF). We performed a set of numerical simulations of 20 000 particles that were originally localized at $H = 1$ in the right well [Fig. 5(a)]. Particles start as a relatively narrow distribution in the right well (black curve). Scattering on resonances causes the maximum of the curve to move to the right, while the distributions become wider. When particles arrive at the top of the hill between the wells (red curve), they immediately start dropping into the left well. After a characteristic time of one full slow period, the distribution becomes essentially uniform in the two bottom wells. There are two characteristic times of the system: the period of the cell T_C and the characteristic time of mixing T_M. Period T_C is defined by the rate of drift $\langle \Delta H \rangle$ and the probability of trapping, $\Pi(H)$ computed at $H = H_{lr}$. The rate of mixing T_M is defined by the second moment of $\langle \Delta H \rangle$,

$$T_C \approx 2\int_{H_{\min}}^{H_C} T(H)\frac{dH}{\langle \Delta H \rangle} + \frac{1}{\Pi(H = H_{lr})}\int_{H_{\min}}^{H_{lr}} T(H)\frac{dH}{\langle \Delta H \rangle},$$

$$T_M \approx 2T(H)\frac{(H_C - H_{\min})^2}{\langle (\Delta H)^2 \rangle}, \tag{4}$$

where $T(H)$ is the period of motion on the (y, p) phase plane. The first term in T_C (approximately equal to 850) is a time over which the drift takes a particle from the bottom of the right well to the bottom of the left well. The second term (approximately equal to 1000) is defined as the time a particle spends near the bottom of the left well before it gets into the L-R trapping.

The drift and diffusive spreading described above create an essentially uniform mixing in the two bottom wells. Beyond that, over a significantly longer timescale, more and more particles diffuse higher into the upper domain, farther away from the separatrix. As a result, they stay there longer, creating a significant population. To estimate the rate of transfer into the upper well, we can use the diffusion-type evolution equation for $\Psi(H, t)$. Numerical simulations indicate that the characteristic timescales of the diffusion into the upper domain are much longer than the timescales of the uniformization in the bottom wells. Thus we can assume that particles are uniformly distributed over the two bottom wells. Trapping into resonance does not occur in the upper domain, and dynamics is determined entirely by scattering on resonance. Scattering on resonance cause a random walk in terms of H. In the upper domain, $\langle \Delta H \rangle = 0$. For any random walk, the diffusion coefficient is equal to one half of the second moment of the corresponding distribution of the magnitude of a single step. On each period, there are two resonance crossings with the same statistical properties. We obtain $D(H) = \langle (\Delta H)^2 \rangle$, and the evolution of $\Psi(H, t)$ can be described by a diffusion-type partial differential equation (PDE),

$$\frac{\partial \Psi}{\partial t} T(H) = \frac{\partial}{\partial H}\left(D(H)\frac{\partial \Psi}{\partial H} \right). \tag{5}$$

The values of $D = D(H)$ are much larger for $H_C < H < H_C + u^2/2 = 13$, where trajectories intersect the resonance four times on a period (including two crossings near $y = 0$), than for $H > H_C + u^2/2$ (two resonance crossings, away from $y = 0$) [see Fig. 1(b)]. Essentially, we can set $D(H < H_C + u^2/2) = \infty$ (uniform mixing) and explicitly study the domain $H > H_C + u^2/2$ only. We compared the predictions of (5) with results of the explicit simulation of 20 000 particles governed by (1). Figure 5(b) presents the amount of particles in the upper domain above $H = 15$. One can see that the PDF-based description describes the leaking of particles into the upper domain.

In conclusion, we considered a motion of charged plasma particles in a nonuniform background magnetic field in the presence of an electrostatic wave. We proposed a setting where the nonlinear resonance creates a large-scale convection cell in phase space. We showed that a combination of the energy drift due to scattering at resonance and trapping

(capture) at resonance creates a regular energy drift, while scattering at resonance creates energy diffusion and mixing. We estimated a characteristic period of the cell and characteristic time of mixing.

F.W. is fully supported by the National Natural Science Fund of China (Award No. 11702331). This material is based in part upon work supported by the National Science Foundation under Award No. CMMI-1740777 (D.V.).

[1] B. Eliasson and P. K. Shukla, Formation and dynamics of coherent structures involving phase-space vortices in plasmas, Phys. Rep. **422**, 225 (2006).

[2] P. Guio, S. Børve, L. K. S. Daldorff, J. P. Lynov, P. Michelsen, H. L. Pécseli, J. J. Rasmussen, K. Saeki, and J. Trulsen, Phase space vortices in collisionless plasmas, Nonlin. Proces. Geophys. **10**, 75 (2003).

[3] F. Zonca, L. Chen, S. Briguglio, G. Fogaccia, G. Vlad, and X. Wang, Nonlinear dynamics of phase space zonal structures and energetic particle physics in fusion plasmas, New J. Phys. **17**, 013052 (2015).

[4] O. Piro and M. Feingold, Diffusion in Three-Dimensional Liouvillian Maps, Phys. Rev. Lett. **61**, 1799 (1988).

[5] M. Feingold, L. Kadanoff, and O. Piro, Passive scalars, 3-dimensional volume-preserving maps, and chaos, J. Stat. Phys. **50**, 529 (1988).

[6] J. Cartwright, M. Feingold, and O. Piro, Global Diffusion in a Realistic Three-Dimensional Time-Dependent Nonturbulent Fluid Flow, Phys. Rev. Lett. **75**, 3669 (1995).

[7] H. Aref *et al.*, Frontiers of chaotic advection, Rev. Mod. Phys. **89**, 025007 (2017).

[8] J. M. Albert, X. Tao, and J. Bortnik, Aspects of nonlinear wave-particle interactions, in *Dynamics of the Earth's Radiation Belts and Inner Magnetosphere*, edited by D. Summers, I. U. Mann, D. N. Baker, and M. Schulz (American Geophysical Union, Washington, DC, 2013).

[9] Y. Omura, D. Nunn, and D. Summers, Generation processes of whistler mode chorus emissions: Current status of nonlinear wave growth theory, in *Dynamics of the Earth's Radiation Belts and Inner Magnetosphere* (Ref. [8]).

[10] N. M. Kroll, P. L. Morton, and M. N. Rosenbluth, Free-electron lasers with variable parameter wigglers, IEEE J. Quantum Electron. **17**, 1436 (1981).

[11] A. Osmane, D. L. Turner, L. B. Wilson, A. P. Dimmock, and T. I. Pulkkinen, Subcritical growth of electron phase-space holes in planetary radiation belts, Astrophys. J. **846**, 83 (2017).

[12] A. V. Artemyev, A. I. Neishtadt, D. L. Vainchtein, A. A. Vasiliev, I. Y. Vasko, and L. M. Zelenyi, Trapping (capture) into resonance and scattering on resonance: Summary of results for space plasma systems, Commun. Nonlin. Sci. Numer. Simul. **65**, 111 (2018).

[13] T. O'Neil, Collisionless damping of nonlinear plasma oscillations, Phys. Fluids **8**, 2255 (1965).

[14] R. K. Mazitov, Damping of plasma waves, J. Appl. Mech. Tech. Phys. **6**, 22 (1965).

[15] F. Valentini, P. Veltri, and A. Mangeney, Magnetic-field effects on nonlinear electrostatic-wave Landau damping, Phys. Rev. E **71**, 016402 (2005).

[16] I. Y. Dodin and N. J. Fisch, Adiabatic nonlinear waves with trapped particles. III. Wave dynamics, Phys. Plasmas **19**, 012104 (2012).

[17] D. Bénisti, Nonlocal adiabatic theory. I. The action distribution function, Phys. Plasmas **24**, 092120 (2017).

[18] X. Tao, F. Zonca, and L. Chen, Identify the nonlinear wave-particle interaction regime in rising tone chorus generation, Geophys. Res. Lett. **44**, 3441 (2017).

[19] A. Neishtadt, A. Vasiliev, and A. Artemyev, Resonance-induced surfatron acceleration of a relativistic particle, Moscow Math. J. **11**, 531 (2011).

[20] A. P. Itin, A. I. Neishtadt, and A. A. Vasiliev, Captures into resonance and scattering on resonance in dynamics of a charged relativistic particle in magnetic field and electrostatic wave, Physica D **141**, 281 (2000).

[21] A. I. Neishtadt, On adiabatic invariance in two-frequency systems, in *Hamiltonian Systems with Three or More Degrees of Freedom*, edited by C. Simo, NATO ASI Series C: Mathematical and Physical Sciences (Kluwer Academic, Dordrecht, 1999), Vol. 533, p. 193.

[22] A. Neishtadt, Passage through a separatrix in a resonance problem with a slowly-varying parameter, J. Appl. Math. Mech. **39**, 594 (1975).

[23] V. I. Arnold, V. V. Kozlov, and A. I. Neishtadt, *Mathematical Aspects of Classical and Celestial Mechanics*, 3rd ed., Encyclopedia of Mathematical Sciences (Springer, New York, 2006).

[24] A. V. Artemyev, A. A. Vasiliev, D. Mourenas, A. I. Neishtadt, O. V. Agapitov, and V. Krasnoselskikh, Probability of relativistic electron trapping by parallel and oblique whistler-mode waves in Earth's radiation belts, Phys. Plasmas **22**, 112903 (2015).

[25] A. V. Artemyev, A. I. Neishtadt, A. A. Vasiliev, and D. Mourenas, Probabilistic approach to nonlinear wave-particle resonant interaction, Phys. Rev. E **95**, 023204 (2017).